Electronic Supplementary Material (ESI) for Physical Chemistry Chemical Physics

Supporting information

Synergistic Increase of Oxygen Reduction Favourable Fe-N Coordination Structures in a Ternary Hybrid Composite of Carbon Nanosphere/Carbon Nanotube/Graphene Sheet

Shiming Zhang[a], *Bin Liu*[b]*, *Shengli Chen*[a]*

[a] *Hubei Key Laboratory of Electrochemical Power Sources, Key Laboratory of Analytical Chemistry for Biology and Medicine (Ministry of Education), Department of Chemistry, Wuhan University, Wuhan 430072, China. Fax: 027-68754693; Tel: 027-68754693; E-mail: slchen@whu.edu.cn*

[b] *School of Chemical and Biomedical Engineering, Nanyang Technological University, 62 Nanyang Drive, Singapore. Fax: 0065-637459; Tel: 0065-637459; E-mail: liubin@ntu.edu.sg*

Contents

S1. Preparation of graphene oxide

Graphene oxide (GO) was synthesized from graphite powder (Sigma Aldrich) using a modified Hummer's method as described previously.[1] Briefly, 2 g of graphite and 1 g KNO_3 were placed in a three-neck flask followed by adding 100 mL concentrated H_2SO_4. Then, 15 g of $KMnO_4$ was gradually added to the mixture under vigorous agitation and the reaction system was stirred for 24 h at 38 ˚C. The flask was then taken out and 300 mL deionized water was added to the mixture in an ice bath, followed by addition of 10 mL of 30 wt% H_2O_2 to terminate the reaction. In order to purify the product, the centrifuged product was dialyzed for about two weeks until no precipitate was detected upon

addition of a few drops of $BaCl_2$ aqueous solution. Finally, the dialysate was subject to acutely ultrasonic exfoliation and then lyophilized to obtain the fluffy GO powder.

S2. SEM and TEM images of the prepared nanocarbons

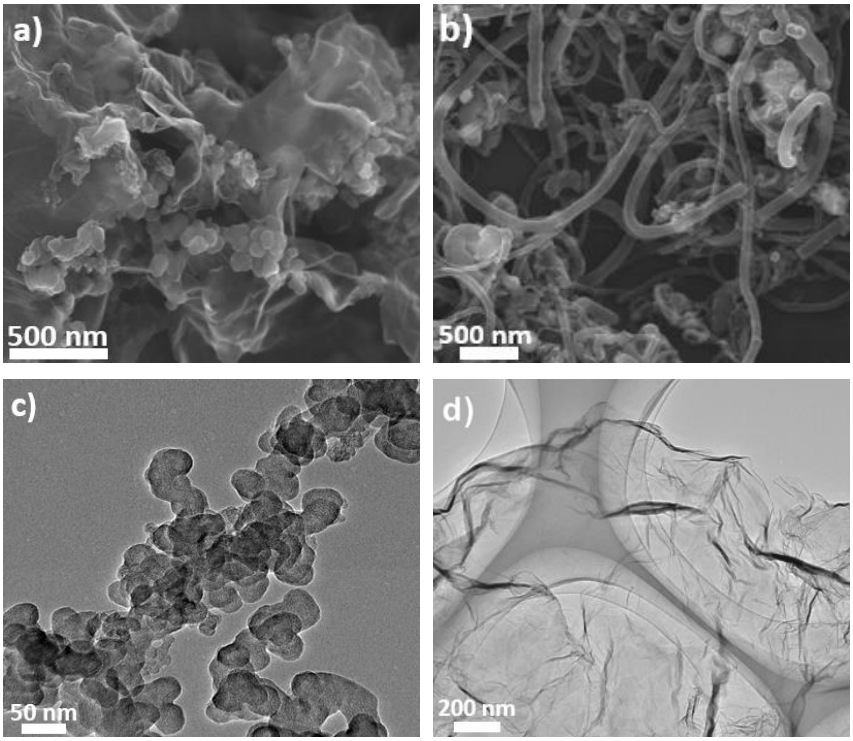

Fig. S1 SEM images of (a) N-CS/GS, (b) FeN-CNT, and TEM images of (c) N-CS, (d) N-GS.

S3. Cyclic voltammograms (CVs) of all the prepared catalysts

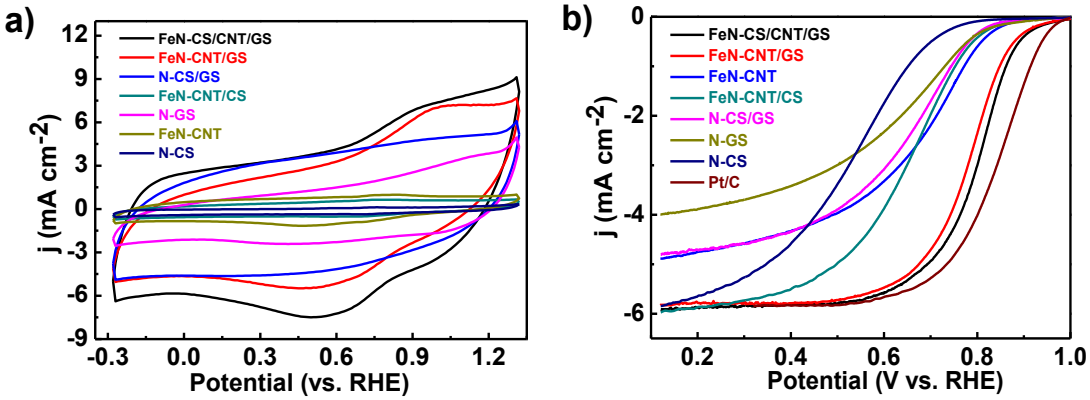

Fig. S2 (a) CVs (100 mV s^{-1}) and (b) ORR polar curves (5 mV s^{-1}) for various samples measured in Ar-saturated 0.1 M $HClO_4$.

S4. Effect of heating temperature, Fe and carbon nanosphere (CS) content in the precursor mixture on ORR activities

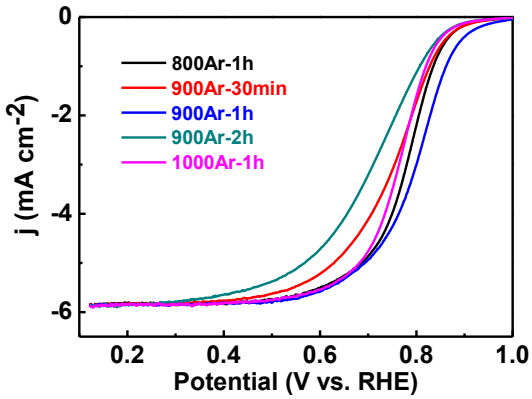

Fig. S3 ORR polarization curves of the ternary FeN-CS/CNT/GS catalysts obtained from precursor composites at different heating temperatures and durations.

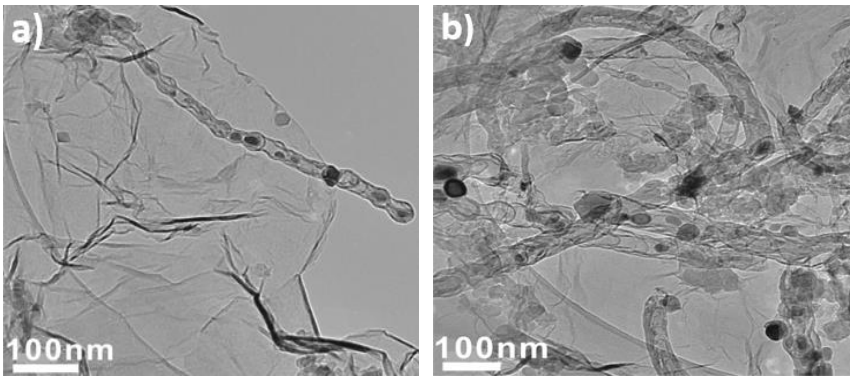

Fig. S4 TEM images of ternary N-CS/CNT/GS catalysts prepared from precursor composites with Fe/GO mass ratios of (a) 1:75 and (b) 1:15.

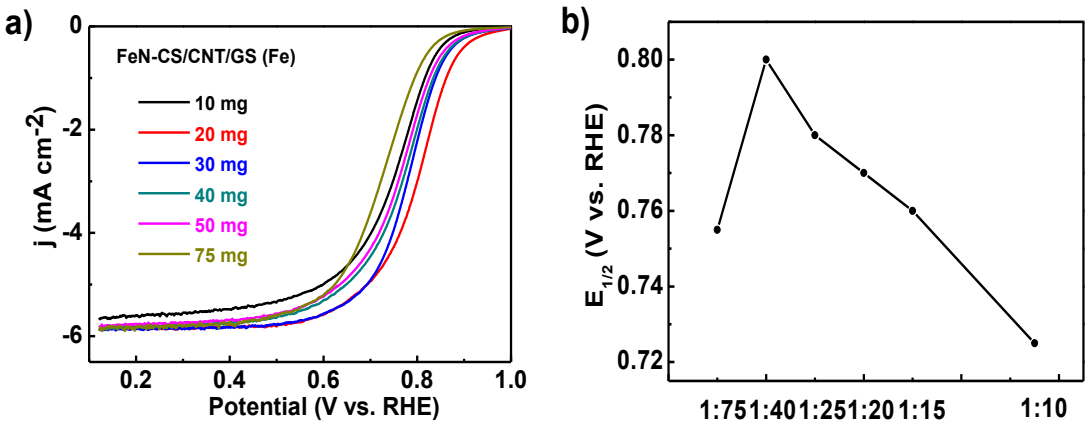

Fig. S5 (a) ORR polarization curves and (b) variation of the half wave potential ($E_{1/2}$) for the FeN-CS/CNT/GS catalysts prepared from precursor composites with different Fe/GO mass ratios.

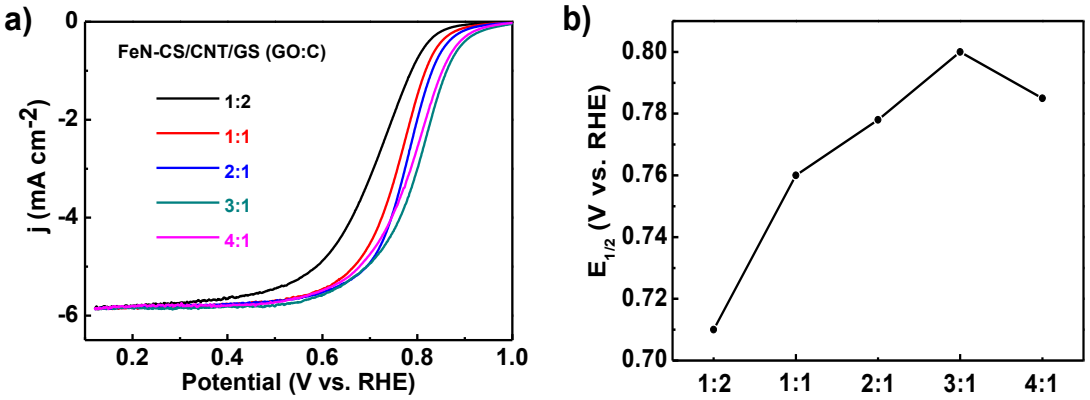

Fig. S6 (a) ORR polarization curves and (b) variation of the half wave potential ($E_{1/2}$) for FeN-CS/CNT/GS catalysts prepared from precursor composites with different GO/C mass ratios.

S5. Additional electrochemical properties of the optimized FeN-CS/CNT/GS composite

Koutecky-Levich analysis. The electron transfer numbers (n) were calculated using Koutecky-Levich equation:[2]

$$i^{-1}=i_k^{-1}+i_l^{-1}=i_k^{-1}+1/(0.62nFAD_{O2}^{2/3}\omega^{1/2}\upsilon^{-1/6}C_O) \quad \text{(eq. S1)}$$

where, i is the measured current; i_k is the kinetic current; i_l is the diffusion-limited current; n is the number of electrons exchanged per mole of O_2; F is the Faraday constant (96500 C mol^{-1}); A is electrode area (0.196 cm^{-2}); D_{O2} is the diffusion coefficient of O_2 in 0.1 M $HClO_4$ solution (2.0×10^{-5} cm^2 s^{-1}); ω is the rotation rate (rad s^{-1}); υ is the kinetic viscosity of water (0.01 cm^2 s^{-1}) and C_O is bulk concentration of O_2 in 0.1 M $HClO_4$ solution (1.2×10^{-6} mol cm^{-3}). The slope of the reciprocal current (i^{-1}) versus the reciprocal square root of rotation rate ($\omega^{-1/2}$) gives n values.

RRDE analysis. The rotating ring-disk electrode (RRDE) measurement was performed on a three-electrode system in O_2-saturated 0.1 M $HClO_4$ solution at a rotation rate of 1600 rpm. The H_2O_2 percentage released during ORR and the apparent electron transfer numbers were calculated using the following equations:[3]

$$n=4I_D/[I_D+(I_R/N)] \quad \text{(eq. S2)}$$

$$H_2O_2\% =200I_R/(N*I_D+I_R) \quad \text{(eq. S3)}$$

where I_D and I_R represent the disk and ring current, respectively, and N is the current collection efficiency of the Pt ring, which was 0.25 in our system.

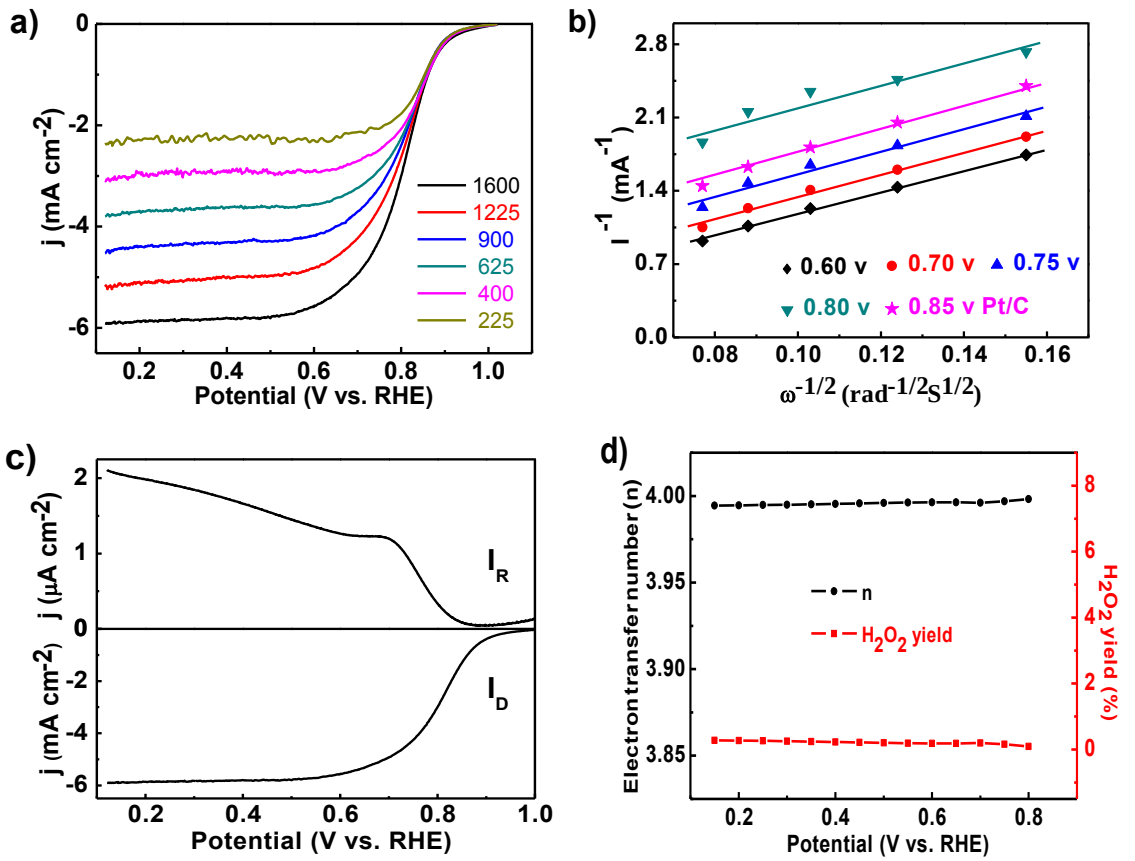

Fig. S7 (a) ORR polar curves of FeN-CS/CNT/GS obtained at different rotating speed in O_2-saturated 0.1 M $HClO_4$; (b) Koutecky-Levich plots at a variety of potentials compared to Pt/C at 0.85 V. (c) Steady-state RRDE experiments and (d) the electron transfer number (n) and H_2O_2 yield of the ternary composite.

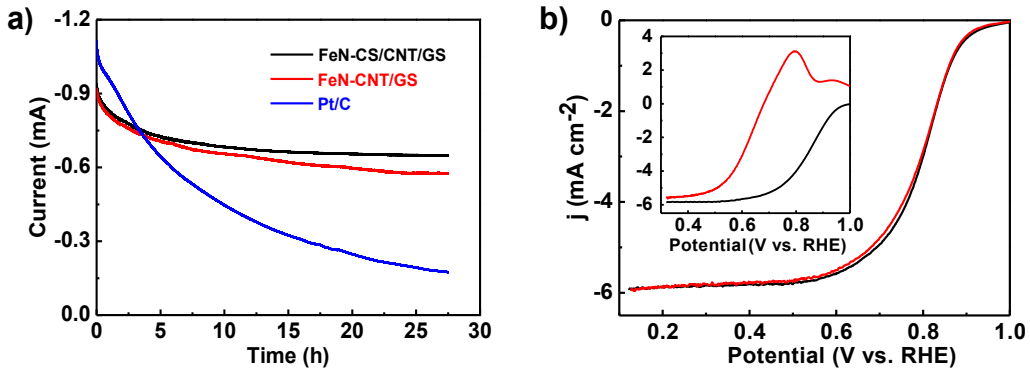

Fig. S8 (a) Current-time curves of FeN-CS/CNT/GS, FeN-CNT/GS, and Pt/C; (b) ORR polarization curves for Pt/C (inset) and FeN-CS/CNT/GS with (red line) and without (black line) addition of 0.1 M methanol.

S6. XPS spectra of N1s

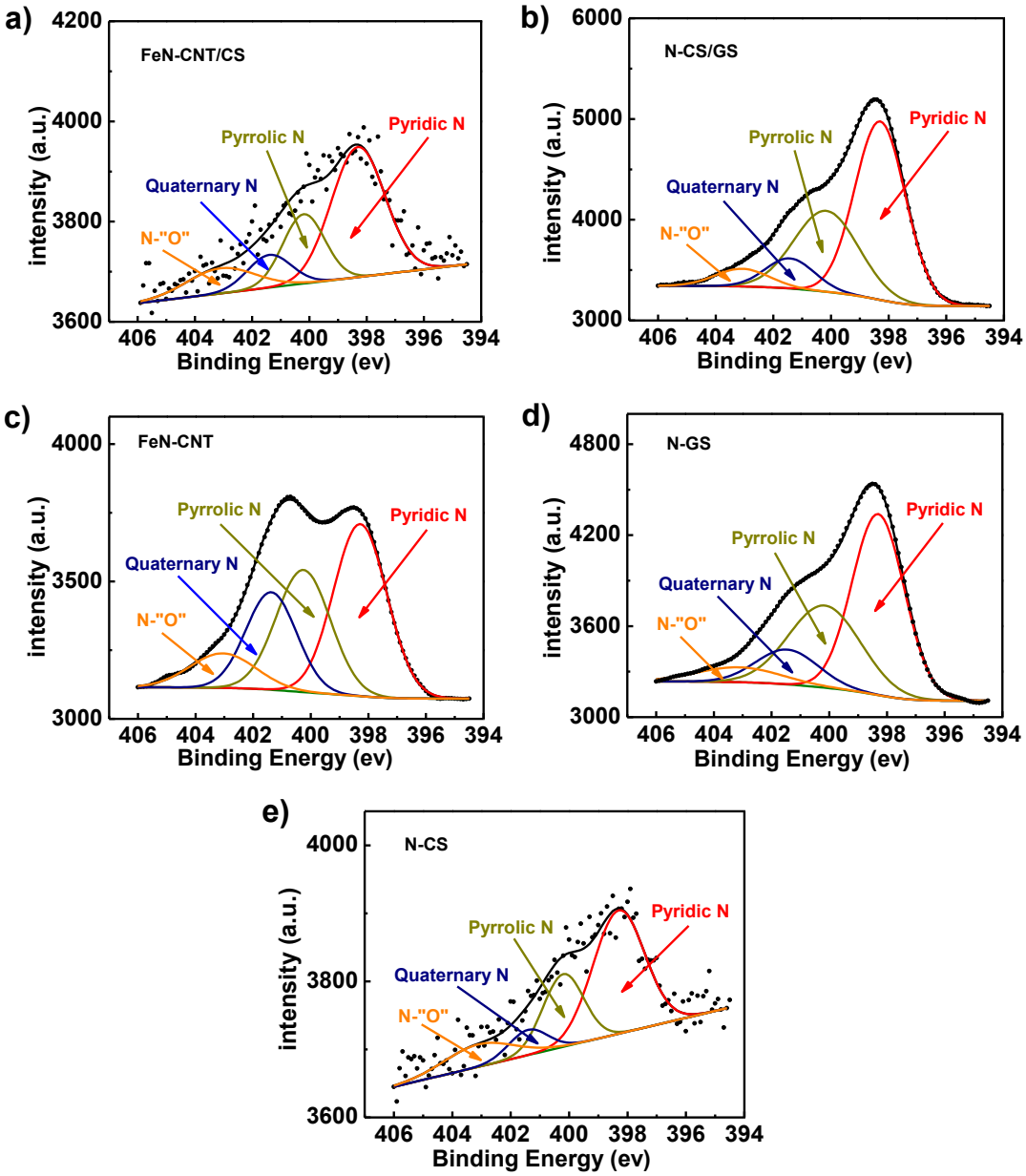

Fig. S9 XPS spectra of N1s and the corresponding deconvolution into components of different N functionalities for (a) FeN-CNT/CS, (b) N-CS/GS, (c) FeN-CNT, (d) N-GS, and (e) N-CS.

S7. Mössbauer results and analysis

Mössbauer spectra were conducted on Oxford Instruments MS 500 with a standard ^{57}Co (Rh) Mössbauer source at the room temperature. Velocity scale and isomer shift δ_{iso} were calibrated against natural iron (α-Fe-foil, 25 μm thick, 99.99% purity) and the δ_{iso} from calibration was used to be the gravity center for the fitting procedure to acquire the accurate Fe nanostructures. The spectroscopic data were analyzed by using the program "Recoil" with the fitting parameters unfixed.

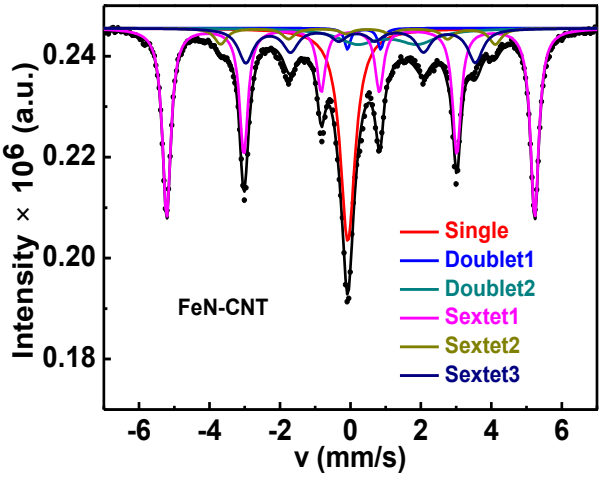

Fig. S10 ^{57}Fe Mössbauer spectra of the FeN-CNT sample.

Singlet:

The singlet found in the ternary and binary composites (δ_{iso} = 0.16 mm s^{-1}) and the FeN-CNT (δ_{iso} = -0.08 mm s^{-1}) may be assigned to a FeN phase observed by Yang. *et al*[4] in the carbon nanotubes encapsulating cubic FeN nanoparticles, or the paramagnetic and superparamagnetic γ-Fe phase reported by Prudnikava. *et al*[5] for the prepared carbon nanotubes.

Doublets:

It may be associated with the C-Fe-N_2 and FeN_4 species for the doublet1 of the ternary composite (δ_{iso} = 0.57 mm s^{-1}, E_Q = 1.41 mm s^{-1}) and the binary composite (δ_{iso} = 0.56 mm s^{-1}, E_Q = 1.44 mm s^{-1}) as well as the doublet 2 of the ternary composite (δ_{iso} = 0.20 mm s^{-1}, E_Q = 2.9 mm s^{-1}) and the binary composite (δ_{iso} = 0.21 mm s^{-1}, E_Q = 2.64 mm s^{-1}). Similar results were reported by Koslowski. *et al*[6] for catalysts with iron porphyrin structures and by Kramm. *et al*[7] when studying catalysts prepared by heating iron porphyrin impregnated on carbon black, respectively.

Furthermore, in FeN-CNT moiety, the doublet1 (δ_{iso} = 0.39 mm s^{-1}, E_Q = 0.94 mm s^{-1}) should be ascribed to the in-plane FeN_4 structures as the catalysts with iron porphyrin structures investigated by Koslowski. *et al*[6], and the catalysts prepared by heating iron porphyrin impregnated on carbon black by Kramm. *et al*[7]. Additionally, the doublet 2 (δ_{iso} = 1.05 mm s^{-1}, E_Q = 1.71 mm s^{-1}) can be associated with C-Fe-N_2 according to its E_Q values.[6, 7]

Sextets:

The sextet1 should be due to the ferromagnetic α-Fe with magnetically split sextet,[5] in the FeN-CS/CNT/GS ternary composite (δ_{iso} = -0.08 mm s^{-1}, E_Q = 0.56 mm s^{-1}, H_0 = 31.01 T) and FeN-CNT/GS binary composite (δ_{iso} = -0.01 mm s^{-1}, E_Q = 0.92 mm s^{-1}, H_0 = 31.00 T), also in the FeN-CNT (δ_{iso} = 0.002 mm s^{-1}, E_Q = 0.01 mm s^{-1}, H_0 = 32.4 T)

The sextet 2 in the ternary and binary composites could be due to $Fe_2C_xN_{1-x}$ phase observed by Yang. *et al*[4] (δ_{iso} = 0.23 mm s^{-1}, E_Q = 0.2 mm s^{-1}, H_0 = 15.9 T) or the Fe_xN which are similar with the results by Borsa. *et al*[8] (δ_{iso} = 0.28 mm s^{-1}, H_0 = 17.9 T). However, for FeN-CNT, it was similar to that of various iron nitrides found by Borsa. *et al*[8] (δ_{iso} = 0.28 mm s^{-1}, H_0 = 24.6 T) and that of nanostructured Fe nitrides obtained by Gajbhiye. *et al*[9] (δ_{iso} = 0.43 mm s^{-1}, E_Q = -0.85 mm s^{-1}, H_0 = 24.78 T). Thus, the sextet 2 in FeN-CNT should be contributed to the Fe nitrides.

Additionally, a sextet 3 has been found in FeN-CNT, which may be explained as the magnetic Fe_5C_2 phase. The almost similar results were observed by Bauer-Grosse *et al*[10] in probing the $Fe_{1-x}C_x$ amorphous alloys and by Tao. *et al*[11] in investigating a precipitated iron-based Fischer-Tropsch synthesis catalyst.

S8. Elemental mapping spectra of the FeN-CNT

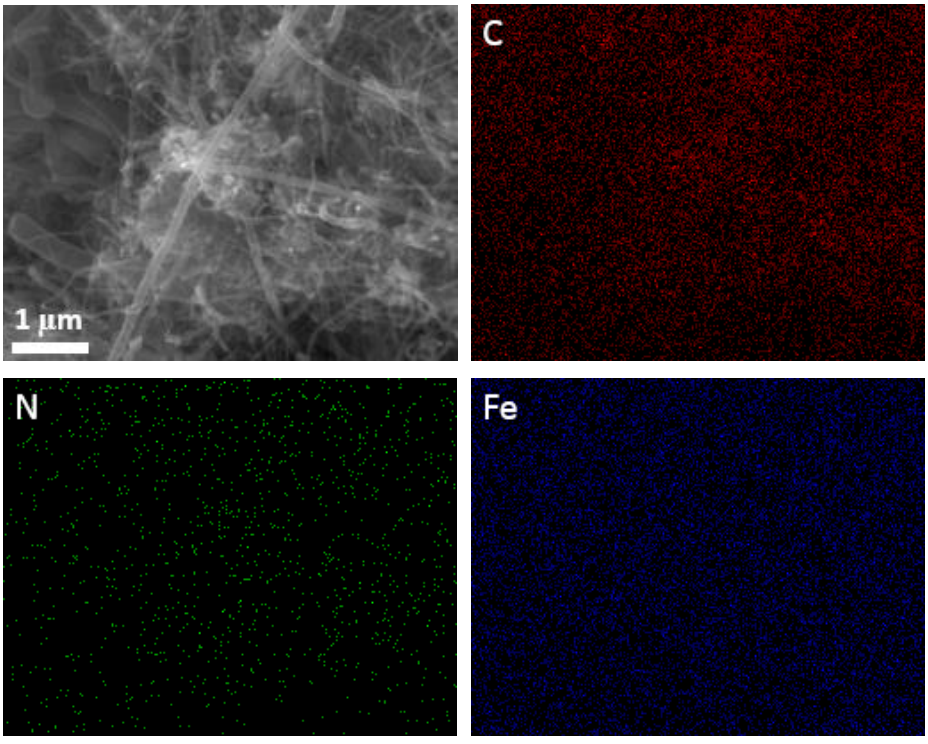

Fig. S11 Elemental mapping spectra of C, N, and Fe for FeN-CNT.

References

1 S. Zhang, H. Zhang, Q. Liu and S. Chen, *J. Mater. Chem. A*, 2013, **1**, 3302-3308.

2 S. Yoshimoto, J. Inukai, A. Tada, T. Abe, T. Morimoto, A. Osuka, H. Furuta and K. Itaya, *J. Phys. Chem. B*, 2004, **108**, 1948-1954.

3 Z.-S. Wu, S. Yang, Y. Sun, K. Parvez, X. Feng and K. Müllen, *J. Am. Chem. Soc.*, 2012, **134**, 9082-9085.

4 Z. Yang, S. Guo, X. Pan, J. Wang and X. Bao, *Energy Environ. Sci*., 2011, **4**, 4500-4503.

5 A. L. Prudnikava, J. A. Fedotova, J. V. Kasiuk, B. G. Shulitski and V. A. Labunov, *Semiconductor Physics, Quantum Electronics & Optoelectronics.*, 2010, **13**, 125-131.

6 U. I. Koslowski, I. Abs-Wurmbach, S. Fiechter and P. Bogdanoff, *J. Phys. Chem. C*, 2008, **112**, 15356-15366.

7 U. I. Kramm, I. Abs-Wurmbach, I. Herrmann-Geppert, J. Radnik, S. Fiechter and P. Bogdanoff, *J. Electrochem. Soc.*, 2011, **158**, 69-78.

8 D. M. Borsa and D. O. Boerma, *Hyperfine Interact.*, 2003, **151/152**, 31-48.

9 N. S. Gajbhiye, R. N. Panda, R. S. Ningthoujam and S. Bhattacharyya, *phys. stat. Sol.*, 2004, **12**, 3252-3259.

10 E. Bauer-Grosse, G. Le Caër and L. Fournes, *Hyperfine Interactions*., 1986, **27**, 297-300.

11 Z. Tao, Y. Yong, C. Zhang, T. Li, M. Ding, H. Xiang and Y. Li, *J. Natural Gas Chem.*, 2007, **16**, 278-285.